The Plant Cell, Vol. 11, 43–55, January 1999, www.plantcell.org © 1999 American Society of Plant Physiologists

# The *IMMUTANS* Variegation Locus of Arabidopsis Defines a Mitochondrial Alternative Oxidase Homolog That Functions during Early Chloroplast Biogenesis

**Dongying Wu,[a,b,1] David A. Wright,[b,c,1] Carolyn Wetzel,[a] Daniel F. Voytas,[b,c] and Steven Rodermel[a,b,2]**

[a] Department of Botany, Iowa State University, Ames, Iowa 50011
[b] Interdepartmental Genetics Program, Iowa State University, Ames, Iowa 50011
[c] Department of Zoology and Genetics, Iowa State University, Ames, Iowa 50011

**Nuclear gene–induced variegation mutants provide a powerful system to dissect interactions between the genetic systems of the nucleus–cytoplasm, the chloroplast, and the mitochondrion. The *immutans* (*im*) variegation mutation of Arabidopsis is nuclear and recessive and results in the production of green- and white-sectored leaves. The green sectors contain cells with normal chloroplasts, whereas the white sectors are heteroplastidic and contain cells with abnormal, pigment-deficient plastids as well as some normal chloroplasts. White sector formation can be promoted by enhanced light intensities, but sectoring becomes irreversible early in leaf development. The white sectors accumulate the carotenoid precursor phytoene. We have positionally cloned *IM* and found that the gene encodes a 40.5-kD protein with sequence motifs characteristic of alternative oxidase, a mitochondrial protein that functions as a terminal oxidase in the respiratory chains of all plants. However, phylogenetic analyses revealed that the IM protein is only distantly related to these other alternative oxidases, suggesting that IM is a novel member of this protein class. We sequenced three alleles of *im*, and all are predicted to be null. Our data suggest a model of variegation in which the IM protein functions early in chloroplast biogenesis as a component of a redox chain responsible for phytoene desaturation but that a redundant electron transfer function is capable of compensating for IM activity in some plastids and cells.**

## INTRODUCTION

Variegation mutants have played a prominent role in the history of genetics (reviewed in Granick, 1955). As a notable example, they were used by E. Bauer in his seminal studies in the early 1900s to describe the phenomenon of non-Mendelian inheritance. The cells in the green sectors of these plants have morphologically normal chloroplasts, whereas cells in the white sectors have abnormal plastids deficient in pigments and organized lamellar structures. One common mechanism of variegation involves the induction of defective mitochondria or chloroplasts in some but not all cells by mutations in nuclear genes (Tilney-Bassett, 1975). Because the products defined by these genes are required for normal chloroplast biogenesis, they provide an excellent starting point to dissect the poorly understood pathways of communication between the nuclear–cytoplasmic, chloroplast, and mitochondrial genetic systems (Taylor, 1989).

Several well-known examples of variegated plants induced by nuclear gene mutations include the maize *iojap* and nonchromosomal stripe (*NCS*) mutants (e.g., Walbot and Coe, 1979; Roussell et al., 1991; Han et al., 1992; Gu et al., 1993) and the barley *albostrians* mutant (e.g., Hess et al., 1994). Both *iojap* and *albostrians* are recessive and give rise to defective, maternally inherited plastids that undergo sorting out to form clonal sectors of affected (white) cells. In both mutants, the plastid defect is traceable to a loss of chloroplast ribosomes and an inability to synthesize chloroplast DNA–encoded components of the photosynthetic apparatus. *IOJAP* has been cloned and sequenced and encodes a protein that is associated with the 50S subunit of the chloroplast ribosome (Han et al., 1992; Han and Martienssen, 1995). Like *iojap* and *albostrians*, *NCS* mutants are recessive. They condition alterations in the mitochondrial genome that generate permanently defective, maternally inherited mitochondria that presumably sort out to form clones of cells containing either all-defective or all-normal mitochondria (e.g., Lauer et al., 1990). Green and white sectors can be observed in *NCS* mutants because the defective mitochondria secondarily affect chloroplast form and function.

Despite the wealth of Arabidopsis mutants, only a handful of nuclear loci have been described that give rise to a variegation phenotype. These include *var1* and *var2* (Martínez-Zapater, 1992), *chloroplast mutator* (Rédei, 1973; Martínez-Zapater et al., 1992; Sakamoto et al., 1996), and *immutans*

[1] These authors contributed equally to this work.
[2] To whom correspondence should be addressed. E-mail rodermel@iastate.edu; fax 515-294-1337.

(*im*; Rédei, 1963, 1967; Röbbelen, 1968; Wetzel et al., 1994; Meehan et al., 1996; Wetzel and Rodermel, 1998). Excluded from this list are alleles of a number of genes that have been transposon tagged by various mutagens (e.g, *Activator*) and that sector because of rounds of element insertion and excision. Of the "natural" variegation loci, only *chloroplast mutator* and *im* have been characterized to an appreciable extent. Like *NCS*, *chloroplast mutator* is recessive and promotes mitochondrial DNA rearrangements that result in permanently defective, maternally inherited mitochondria; chloroplast phenotype is affected secondarily (Martínez-Zapater et al., 1992; Sakamoto et al., 1996).

*im* (Figure 1) is also recessive, but in contrast to *chloroplast mutator*, sectoring is sensitive to light intensity and temperature: elevated light or temperature results in an increase in white sector formation (Rédei, 1963; Röbbelen, 1968). Rédei (1963, 1975) also found that pure-white reproductive bolts of *im* can give rise to all-green, all-white, or variegated progeny, depending on the light and temperature growth regimes of the progeny. Because of the apparent reversibility of the phenotype and an inability of the mutant to convert permanently from a normal green to an all-white phenotype, Rédei (1975) called the mutation *im*, from a Latin word meaning immutable.

We originally became interested in *im* because we felt that it might provide information about the pathways of interorganellar communication. To this end, we have examined plastid morphology and inheritance, analyzed pigment compositions, and examined patterns of nuclear and chloroplast gene expression in the mutant (Wetzel et al., 1994; Meehan et al., 1996; Wetzel and Rodermel, 1998). We found that the *im*-conferred phenotype is first expressed during early germination and that white tissues of the mutant can be heteroplastidic for cells that contain abnormal and normal-appearing plastids. Heteroplastidic cells are a rare phenomenon in plants, because plastids typically sort out rapidly to form clones of pure-white and pure-green cells (i.e., homoplastidic cells) (Tilney-Bassett, 1975). The finding of heteroplastidic cells indicates that *im* is "plastid autonomous" and that the gene product defined by the mutation has an unequal effect on the plastids in a cell. We also found that white *im* sectors accumulate the carotenoid precursor phytoene but that *IM* is not the structural gene for phytoene desaturase (PDS), the enzyme that converts phytoene to ζ-carotene in the plastid (Bartley et al., 1991; Wetzel et al., 1994). We further observed that PDS mRNA and protein levels are normal in the mutant (Wetzel and Rodermel, 1998), indicating that IM does not directly affect *PDS* expression. One possibility we suggested is that IM could be a cofactor required for maximal PDS activity (Wetzel et al., 1994). The phenotype of the *im* mutant is very similar to that of the *ghost* variegation mutant of tomato (e.g., Scolnik et al., 1987; Giuliano et al., 1993), and the two mutants may have defects in homologous genes.

In this study, we report the positional cloning of *IM*, and we define the nature of the mutations in three *im* alleles, including two x-ray–induced alleles that were generated by Rédei nearly 50 years ago. We also show that the IM protein is related to alternative oxidase (AOX), an inner mitochondrial membrane protein that functions as a terminal oxidase in the respiratory chains of all plants and of some algae, fungi, and protists.

**Figure 1.** An Arabidopsis Mutant Carrying the *spotty* Allele of *im.*

The green sectors contain normal-appearing chloroplasts, whereas the white sectors are heteroplastidic for abnormal plastids lacking pigments and lamellar structures as well as for rare normal chloroplasts (Wetzel et al., 1994). The white sectors accumulate the carotenoid precursor phytoene (Wetzel et al., 1994), and white sector formation is promoted by increased light intensity (Rédei, 1963; Röbbelen, 1968).

## RESULTS

### Positional Cloning of *IM*

*IM* resides within an ~9.6-centimorgan (cM) interval on chromosome 4 between *cer2* and *ag* (Wetzel et al., 1994) (Figure 2A). To initiate a chromosome walk to the gene, we generated an $F_2$ mapping population by performing crosses between a line carrying the *spotty* allele of *im* (in the Columbia ecotype background) (Wetzel et al., 1994) and a Landsberg *erecta* chromosome 4 marker line (*cer2*/*ap2*/*bp2*) (Koornneef et al., 1983). Early in the walk, there was a dearth of physical information on chromosome 4, and $F_2$ plants were screened for recombination breakpoints in the *bp–im* and *im–cer2* intervals on the basis of phenotype. However, as more physical information became available, we were able to screen recombinant $F_2$ plants rapidly by using markers *nga1111* and *nga1139*, which encompass *im* within an ~40-cM interval (Figure 2B) (Bell and Ecker, 1994).

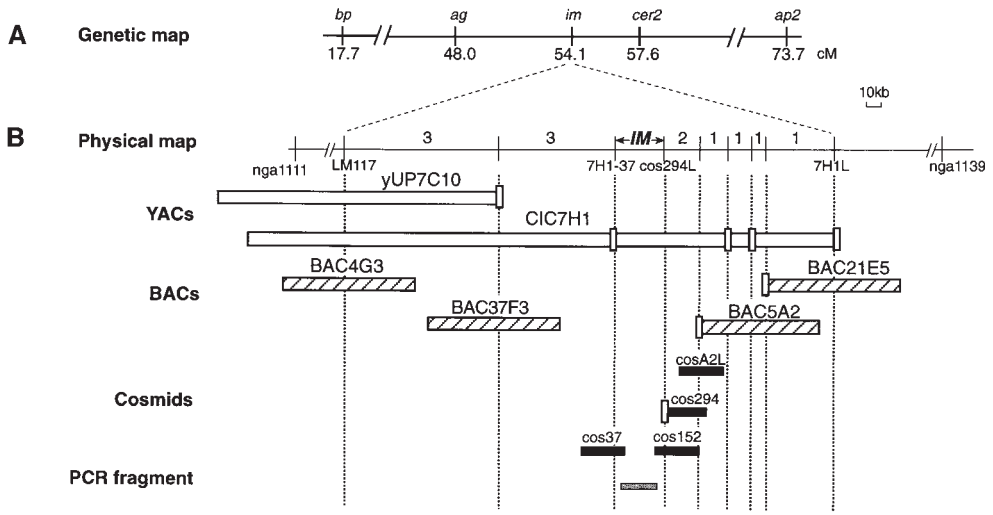


**Figure 2.** Positional Cloning of *im.*

**(A)** Genetic map. *im* maps between *cer2* and *ag* on chromosome 4 (Rédei, 1967; Wetzel et al., 1994).
**(B)** Physical map. The physical contig encompassing *im* extends from restriction fragment length polymorphism marker LM117 to cleaved amplified polymorphic sequence (CAPS) marker 7HIL, which represents a distance of ~320 kb. CAPS markers 7H1-37 and cos294L cosegregate with *im.* Two of six yeast artificial chromosomes (YACs) in the *im* contig are shown; this is part of an extended 17-Mb YAC contig in this region of chromosome 4 (Schmidt et al., 1996). Bacterial artificial chromosomes (BACs) and cosmid clones in the immediate vicinity of *im* are shown. End clones that were isolated and converted into CAPS markers are designated by rectangles on the clone diagrams. The number of recombinant chromosomes between markers is indicated. A total of 2495 $F_2$ plants (4990 chromosomes) were analyzed to generate the recombinant population.

We identified a restriction fragment length marker that mapped close to *im* (LM117; ~0.12 cM), and this marker served as the starting point for the walk (Figure 2B). This marker was used to detect a series of overlapping yeast artificial chromosomes (YACs), which were then mapped with respect to *im* by using cleaved amplified polymorphic sequence (CAPS) markers (Konieczny and Ausubel, 1993). The CAPS markers were generated from YAC end clones as well as from random EcoRI fragments of YAC CIC7H1. By using this analysis, we were able to determine that YAC CIC7H1 completely encompasses *im.* The YAC-derived markers also were used to isolate a series of overlapping bacterial artificial chromosomes (BACs) and cosmid clones that immediately flank *im.* BAC and cosmid end clones were then isolated, and CAPS markers were generated. These were used to fine-map recombination breakpoints within the vicinity of *im.* We were unable to isolate cosmids or plasmids that overlapped *im.* This was due to a sequence immediately downstream from the gene that caused clone instability in *Escherichia coli* (data not shown). The region encompassing *im* was finally overlapped by a long polymerase chain reaction (PCR) product (24 kb) generated with primers based on *cos37* and *cos152* DNA sequences (Figure 2B).

To localize *im* within the long PCR product, we digested the PCR product with SalI and SacI and cloned the fragments into pBluescript. Using the cloned fragments as probes, we conducted genomic DNA gel blot experiments to detect polymorphisms between DNAs from various *im* alleles and wild-type Columbia DNA. Rédei's initial studies with *im* were based on the x-ray–induced *im-1* allele (Rédei, 1963, 1967). A 3.1-kb SalI-SacI subfragment of the long PCR product detected a 3.4-kb EcoRI fragment in the wild-type DNA that was shifted to a smaller 2.5-kb EcoRI fragment in *im-1* DNA (data not shown). This 3.4-kb fragment was used as a probe to isolate four different-sized cDNAs from an Arabidopsis cDNA library (Newman et al., 1994). This library contained sequences from developmental stages when we would anticipate *IM* to be expressed (Wetzel and Rodermel, 1998). The cDNAs were sequenced and found to be derived from a single gene. This is consistent with low-stringency genomic DNA gel blot analyses showing that *IM* is most likely a single-copy gene in Arabidopsis (data not shown). The sequence of the longest of the four cDNAs (1.4 kb) was compared with that of the wild-type genomic sequence, and a gene with nine exons was identified (Figure 3A). We were unable to detect a transcript for this gene on gel blots using RNA from a variety of tissues and developmental stages when we would expect *IM* to be expressed (Wetzel and Rodermel, 1998), indicating that the gene is expressed at very low levels.

The candidate *IM* gene was contained completely within the 3.4-kb EcoRI fragment identified by our probe in wild-type DNA (Figure 3B). To characterize the rearrangement in

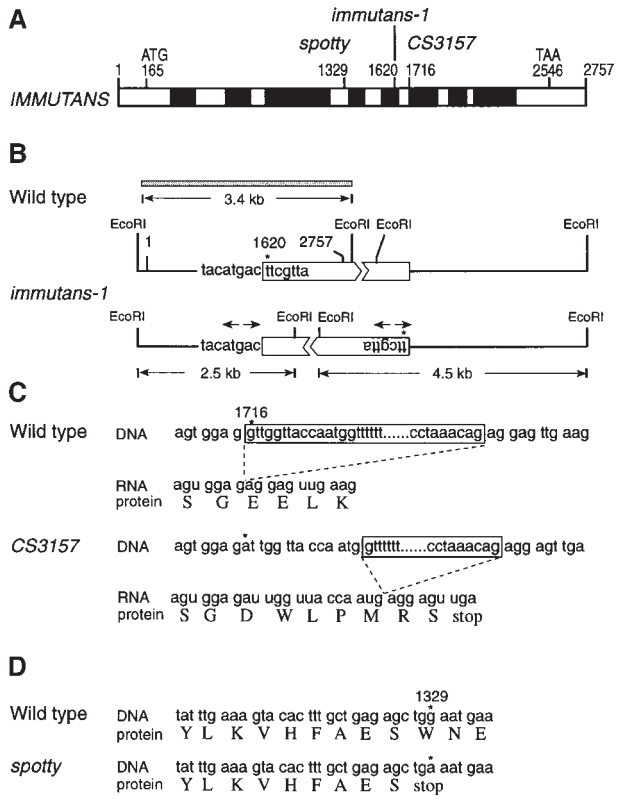


**Figure 3.** Mutations in *im* Alleles.

**(A)** Schematic representation of the *IM* genomic sequence. *IM* is composed of nine exons (white) and eight introns (shaded). The transcription start site is designated as base 1, and the poly(A) addition site is base 2757. Also shown are the presumed translation start (base 165) and stop (base 2546) codons and the locations of the mutations in the three *im* alleles. Immediately downstream of the last exon is a long stretch of simple repeated sequence (data not shown). **(B)** to **(D)** Comparison of the nucleotide and derived amino acid sequences of wild-type and mutant *im* alleles. In **(B)** for *im-1*, a large inversion interrupts the gene, giving rise to EcoRI polymorphic fragments on DNA gel blots. The white box (with the upside-down sequence) represents the inversion, interrupted by greater than ~200 kb of genomic sequence. The shaded box is the probe used in the hybridizations. The arrows above the *im-1* diagram represent the primer pairs used to inverse PCR amplify the 2.5- and 4.5-kb fragments. Wild-type *IM* sequences at the site of the inversion (indicated by an asterisk) are shown. In **(C)** for *CS3157*, there is a G-to-A transition at base 1716 that results in the use of an alternate 5′ splice site in the sixth intron and the generation of a premature stop codon in the seventh exon. Intron sequences are boxed, and dashed lines indicate sequences that are spliced from the precursor to generate the mature mRNA. In **(D)** for *spotty*, there is a G-to-A transition at base 1329 in the fourth exon, generating a nonsense mutation. In **(C)** and **(D)**, the asterisks indicate the wild-type and mutated bases.

the *im-1* line, we designed two PCR primer pairs to amplify, by inverse PCR, the 2.5- and 4.5-kb EcoRI fragments observed on gel blots with *im-1* DNA. The resulting PCR amplification products were sequenced, and an abrupt DNA sequence change was revealed in the fifth intron of the candidate gene (at base pair 1620) compared with the wild type (Figure 3B). In searches of the DNA sequence databases, the novel sequences from both the 2.5- and 4.5-kb EcoRI fragments were found adjacent to one another in BAC F18E5, which contains an insert of chromosome 4 DNA (GenBank accession number AL022603). This BAC lies outside of our contig, which extends ~200 kb on either side of *IM.* Considered together, these data indicate that a very large inversion has occurred on chromosome 4 in the *im-1* strain and that this inversion interrupts a gene whose map position corresponds to *im.*

Two other *im* alleles were characterized to determine whether they carry mutations in the candidate gene. *CS3157* is another x-ray–induced *im* allele that was originally isolated by Rédei. Genomic PCR products of the gene in *CS3157* were sequenced, and a G-to-A transition was identified at the sixth exon/sixth intron boundary (Figures 3A and 3C). Because intron splice sites are conserved in higher plants (Brendel et al., 1998), this change would be predicted to give rise to a splicing defect. This possibility was tested using exon primers that span the mutation to amplify mRNA by reverse transcriptase–PCR (RT-PCR). The DNA sequence of the RT-PCR product showed that the mutation gave rise to an mRNA that was spliced at an alternative downstream 5′ splice site (Figure 3C). This sequence should give rise to a truncated protein, because a premature stop codon is generated immediately downstream of the alternative splice site.

The third *im* allele we examined was *spotty*, which was induced by ethyl methanesulfonate mutagenesis (Wetzel et al., 1994). In *spotty*, we identified a point mutation in the fourth exon of the candidate gene that changes a G to an A (Figures 3A and 3D). This transition converts a tryptophan codon to a stop codon. RT-PCR analyses failed to detect an mRNA species for the candidate gene in the *spotty* background.

In summary, we conclude that we have isolated *IM* on the basis of both the fine-mapping studies and the identification of mutations in a gene from three independent *im* alleles. This conclusion has been confirmed by analysis of *Activator*-tagged mutants of this gene (Carol et al., 1999).

### *IM* Is an AOX Homolog

The largest of the *im* cDNAs that we characterized was 1.4 kb. The 5′ end of the mRNA was identified by 5′ rapid amplification of cDNA ends (5′ RACE) (data not shown); these analyses extended the 5′ end of the cDNA ~60 bp. Figure 4A shows the complete cDNA sequence and deduced amino acid sequence of the IM protein. The amino acid sequence predicts a protein with a calculated molecular mass of 40.5 kD. Database searches revealed that the amino acid

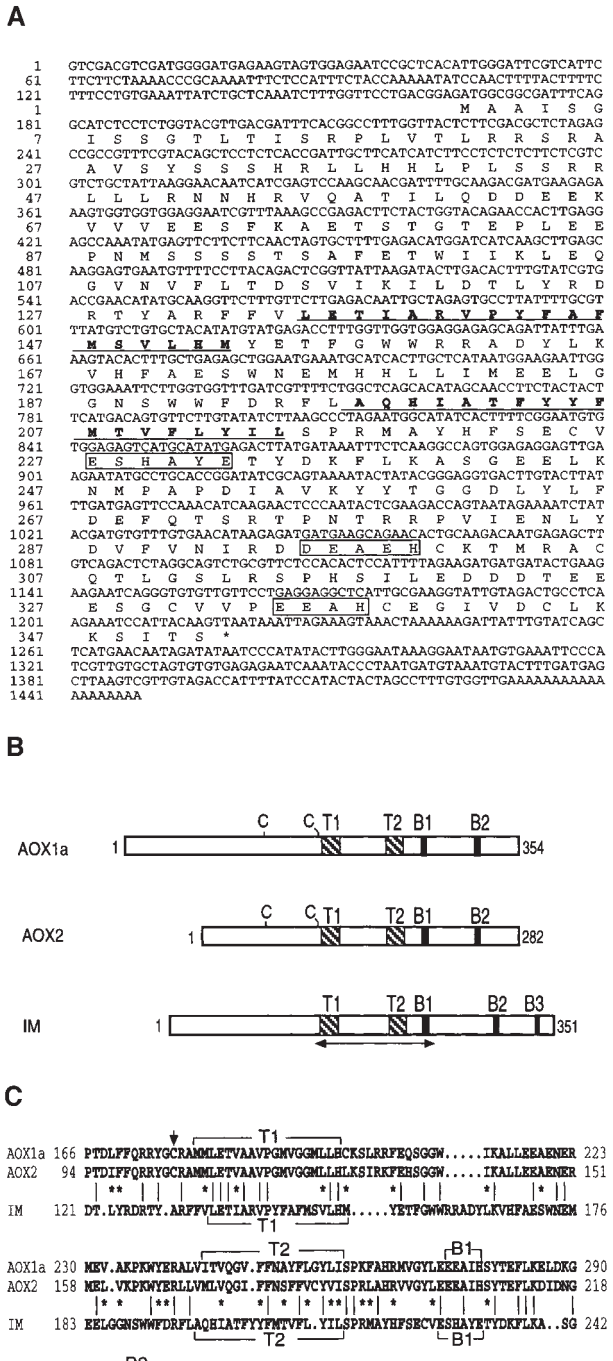


**Figure 4.** *IM* cDNA Sequence and Comparison to AOX Protein Sequences.

**(A)** *IM* cDNA and deduced amino acid sequences. Conserved transmembrane domains are underlined, and conserved iron binding motifs are boxed. The asterisk indicates the stop codon.

sequence bears high similarity to AOXs ($P = 1 \times 10^{-4}$ to $4 \times 10^{-13}$). AOXs are inner mitochondrial membrane proteins found in all higher plants and in some algae, fungi, and protists (Siedow and Umbach, 1995; Vanlerberghe and McIntosh, 1997). Species with AOX have two pathways of respiration: a cyanide-sensitive pathway, whose terminal oxidase is cytochrome *c* oxidase; and a cyanide-resistant, salicylhydroxamic acid–sensitive pathway, whose terminal oxidase is AOX. The two pathways diverge at the ubiquinol pool, with AOX directly transferring electrons from ubiquinol to oxygen.

*AOX* genes typically constitute small nuclear multigene families (Saisho et al., 1997; Vanlerberghe and McIntosh, 1997). In Arabidopsis, for example, there are four *AOX* gene family members, designated *AOX1a*, *AOX1b*, *AOX1c*, and *AOX2* (Kumar and Söll, 1992; Saisho et al., 1997). The deduced amino acid sequences of all *AOX* genes share several conserved domains. These include two α-helical, membrane-spanning domains in the center of the protein and two iron binding motifs in the hydrophilic C-terminal portion of the protein (Siedow and Umbach, 1995; Vanlerberghe and McIntosh, 1997). The latter motifs may form a binuclear iron center (Moore et al., 1995; Siedow et al., 1995). Higher plant AOX proteins also appear to have two conserved cysteine residues that are involved in dimerization and in the regulation of enzyme activity by redox status and pyruvate (Umbach and Siedow, 1993, 1996). One or both of these cysteines is missing in non-plant proteins (Vanlerberghe and McIntosh, 1997).

Figures 4B and 4C show that the conserved domains of higher plant AOX proteins also are conserved in the deduced amino acid sequence of the IM protein; AOX1a and AOX2 from Arabidopsis are used as representative protein sequences for comparison. The regions of similarity include the membrane-spanning domains (T1 and T2). These regions in IM

**(B)** Schematic comparison of the primary amino acid sequences of the IM protein and the Arabidopsis AOX1a and AOX2 proteins (Saisho et al., 1997). T1 and T2 are conserved transmembrane domains; B1, B2, and B3 are iron binding motifs; C denotes conserved cysteine residues. The double-headed arrow indicates sequences used for phylogenetic analyses (Figure 5). The number of amino acids in each protein is indicated at the C terminus.

**(C)** Amino acid sequence comparisons of the conserved regions of the IM protein and the Arabidopsis AOX1a and AOX2 proteins (Saisho et al., 1997). The small brackets indicate the C termini of the AOX1a and AOX2 proteins. Identical amino acids shared by all three sequences are indicated by vertical lines. An asterisk indicates that an IM amino acid is identical to an amino acid in one of the other two sequences at that position or that it is a conservative substitution compared with the other two amino acids at that position (determined by using the BOXSHADE sequence alignment program http://www.isrec.isb-sib.ch/ttp-server/boxshade/MacBoxshade). The arrow designates the conserved cysteines in the AOX1a and AOX2 sequences. Dots indicate gaps that were introduced to optimize the alignment.

were predicted to be part of a transmembrane domain by the PHDhtm program (>80% confidence level) (Rost et al., 1995). In contrast to the derived amino acid sequences of other characterized *AOX* genes, the derived *IM* sequence has homology to three putative iron binding motifs (B1, B2, and B3). The first of these (B1) is located in a comparable position to the AOX B1 motif, but the IM B1 sequence is slightly degenerate. The B2 sequence is highly conserved in position and sequence. The B3 motif, on the other hand, is downstream from where the Arabidopsis AOX1A and AOX2 sequences end. IM also differs from higher plant AOX proteins in that the two conserved cysteines are not present.

In contrast to the C terminus, the N terminus of IM bears little identifiable similarity to other AOX proteins. PSORT software (Nakai and Kanehisa, 1992) predicts that the first 50 amino acids of the protein comprise an N-terminal transit sequence to target IM to the chloroplast. For instance, this region has a high content of serine (22%), no aspartic acid or glutamic acid, and an alanine after the initiating methionine (Cline and Henry, 1996). The presence of a sequence that is capable of targeting IM to the plastid in vitro has been confirmed by Carol et al. (1999).

To further assess relationships between IM and known AOX amino acid sequences, we conducted phylogenetic analyses using the neighbor-joining algorithm (Saitou and Nei, 1987; Felsenstein, 1993) (Figure 5). For tree construction, amino acid sequences were limited to the conserved transmembrane domains and the first two iron binding motifs (double-headed arrow in Figure 4B). *IM* and all plant *AOX* gene sequences were well separated from *AOX* genes of algae, fungi, and protists (in 65% of bootstrap replicates). This suggests that *IM* shares a more recent evolutionary history with plant *AOX* genes. Most plant *AOX* sequences form a single, well-supported clade (95% bootstrap support) (the nine sequences in the bottom of Figure 5). Genes within this branch share ~75 to 95% amino acid identity. Although more distantly related *AOX* genes are found in plants (namely, Arabidopsis *AOX*2, *Glycine max AOX*2 and *AOX*3, and *Mangifera indica AOX*), their relationship to each other and to the other *AOX* genes is less clear. *IM* is distantly related to all plant *AOX* genes (as indicated by its long branch length), including these more divergent *AOX* family members. Thus, even though *IM* shares many conserved structural motifs with plant *AOX* genes, it appears to be a novel type of AOX.

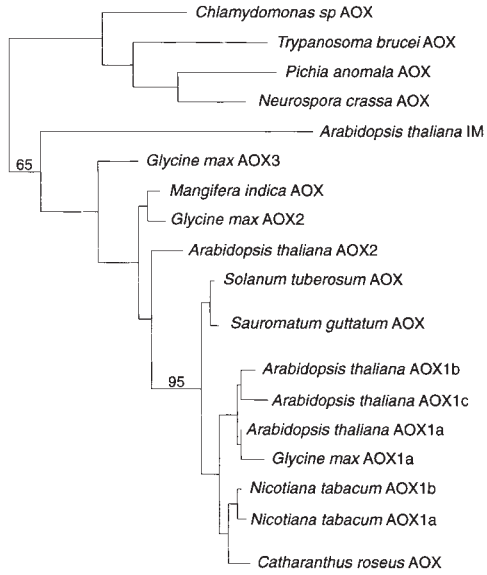


**Figure 5.** Phylogenetic Relationships of AOX and IM Amino Acid Sequences.

Relationships were determined by the neighbor-joining distance algorithm using Phylip (Saitou and Nei, 1987; Felsenstein, 1993). Bootstrap values (100 replicates) are shown for major branches above the branch nodes. Those sequences not described in Saisho et al. (1997) include *AOX* genes from *Solanum tuberosum* (GenBank accession number 1588565), *Catharanthus roseus* (GenBank accession number 2696032), and *Chlamydomonas* sp (GenBank accession number 2662190).

## DISCUSSION

### IM Is a Novel AOX-like Chloroplast Protein

All higher plants have an alternative (cyanide-resistant) pathway of mitochondrial respiration in the inner membrane that branches from the cytochrome pathway at the ubiquinone pool (reviewed in Siedow and Umbach, 1995; Vanlerberghe and McIntosh, 1997). The alternative pathway uses a terminal oxidase (AOX) that generates water from ubiquinol in a four-electron transfer reaction. The alternative pathway does not contribute to the generation of an electrochemical gradient and therefore is not coupled to ATP production. Because AOX is able to compete with the cytochrome pathway for electrons, the alternative pathway does not serve merely as an "energy overflow" mechanism when electron transport through the cytochrome pathway is saturated with electrons, damaged, or restricted by the availability of ADP (Purvis and Shewfelt, 1993; Hoefnagel et al., 1995; Ribas-Carbo et al., 1995; Siedow and Umbach, 1995). Vanlerberghe et al. (1997) have demonstrated that the alternative pathway may play an important role in balancing carbon metabolism and electron transport.

Our data suggest that the *IM* gene product is a member of the AOX class of proteins. Not only does its derived C-terminal sequence bear regions of high similarity to the signature motifs of AOX proteins from diverse sources, but phylogenetic analyses indicate that *IM* is distantly related to all known plant *AOX* genes. On the other hand, the lack of similarity in the N terminus suggests, at a minimum, that if IM

functions as an AOX, then its regulation is likely very different from that of known AOX proteins. For example, IM lacks the two conserved cysteines that are important in dimerization and regulation of AOX activity in higher plants (Umbach and Siedow, 1993, 1996). IM also has three rather than two putative iron binding motifs. Furthermore, our analyses revealed that IM is targeted to the chloroplast rather than the mitochondrion, as is the case with other AOX proteins. This has been confirmed by the demonstration that IM is associated with the membrane fraction of plastids in an in vitro import assay (Carol et al., 1999).

### Mechanism of *im* Variegation

A satisfactory explanation of sector formation in *im* must take into account the following observations.

(1) Ultrastructural analyses have shown that whereas cells in the green sectors contain normal chloroplasts, cells in the white sectors are heteroplastidic for normal-appearing chloroplasts and vacuolated plastids that lack internal lamellar structures (Wetzel et al., 1994). The finding of heteroplastidic cells indicates that the nuclear gene product coded for by *im* has an unequal affect on the plastids in a cell, that is, the mutation is "plastid autonomous" (Wetzel et al., 1994).

(2) White sector formation is promoted by enhanced light intensities (Rédei, 1963; Röbbelen, 1968; Wetzel et al., 1994).

(3) Sector formation during leaf development results in a fixed pigmentation state in *im.* Pure-white and heteroplastidic cells do not become green when placed under low light intensities, and green sectors do not bleach when plants are placed under high light intensities (Wetzel et al., 1994).

(4) *IM* is first expressed in cotyledons during a discrete, light-responsive phase immediately following seed coat breakage. Its expression during this phase determines irreversibly the degree of white and green sector formation in the cotyledons (Wetzel et al., 1994). This suggests that sector formation in leaves is also determined at an early stage of cell development.

(5) The white *im* sectors accumulate phytoene, suggesting that PDS activity is impaired in the white cells (Wetzel et al., 1994). However, PDS mRNA and protein levels are normal in the green and white sectors of the mutant (Wetzel and Rodermel, 1998).

### Role of *IM* in Carotenoid Synthesis: Why Does Phytoene Accumulate?

Accumulation of phytoene in *im* white sectors, where the PDS protein is found at wild-type levels, indicates that PDS is not active in this tissue. The lack of activity is not a generalized result of photooxidation, because a chemically induced block in carotenoid biosynthesis at a later step in the pathway causes bleaching but not accumulation of phytoene (Sandmann and Böger, 1989). Precursor-feeding experiments have revealed that chlorophyll synthesis is not specifically inhibited in *im* (C. Wetzel and S. Rodermel, unpublished data). Thus, the white sectors in mutant leaves are the result of impaired PDS activity leading to a block in carotenoid synthesis. Lack of carotenoids leads secondarily to a loss of chlorophyll, due either to inhibition of its accumulation and/or to its photodestruction.

All of the early steps of carotenoid biosynthesis are mediated by soluble stromal enzymes, but the later steps, that is, those including and subsequent to the desaturation of phytoene, occur on membrane-bound enzymes (e.g., Kreuz et al., 1982; Bonk et al., 1996; Cunningham and Gantt, 1998). These enzymes may form a multisubunit complex. A function of this complex would be to transfer electrons from phytoene to a series of acceptors during the PDS and ZDS (ζ-carotene desaturase) desaturation steps of the pathway. Consistent with this proposal, several redox components have been found to be necessary for PDS activity: plastoquinone (Mayer et al., 1990; Schulz et al., 1993; Nievelstein et al., 1995; Norris et al., 1995), NADPH (Mayer et al., 1992), PDS-bound flavin adenine dinucleotide (Hugueney et al., 1992; Al-Babili et al., 1996), and molecular oxygen (Beyer et al., 1989; Mayer et al., 1990). Also consistent with this proposal are analyses of the redox activities of various artificial quinones. These analyses have suggested that phytoene desaturation involves a multicomponent redox chain between PDS and oxygen (Mayer et al., 1990).

Our finding that IM bears striking homology to AOX suggests that IM may be an electron transfer component of the phytoene desaturation pathway. We have previously suggested that IM may be a cofactor required for PDS activity (Wetzel et al., 1994; Wetzel and Rodermel, 1998). This possibility is illustrated in Figure 6A. In this model, electrons would be transferred from phytoene via PDS to IM and thence to the plastoquinone pool. In the absence of IM, phytoene would be expected to accumulate. However, another possibility is that IM functions like AOX, that is, as a terminal oxidase, and transfers electrons either directly to molecular oxygen (Figure 6A) or in a more indirect manner from PDS to oxygen (Figure 6B). The latter would be consistent with a function of IM as the elusive plastoquinol oxidase in the chlororespiratory chain (e.g., Büchel and Garab, 1997; Burrows et al., 1998; Feild et al., 1998; Kofer et al., 1998; Shikanai et al., 1998). In either of these cases, phytoene might again be predicted to build up in the absence of IM: PDS would be unable to desaturate phytoene (Figure 6A), or the plastoquinone pool could become over-reduced (e.g., in cases in which electron transfer from the plastoquinone pool to photosystem I is limiting; see below), thus preventing the transfer of electrons from PDS to plastoquinone (Figure 6B). Although the models in Figure 6 have placed IM-related electron transport in the context of the photosynthetic electron transport chain via the plastoquinone pool, it is possible that a portion of the pathway exists in the inner envelope (Jäger-Vottero et al., 1997).

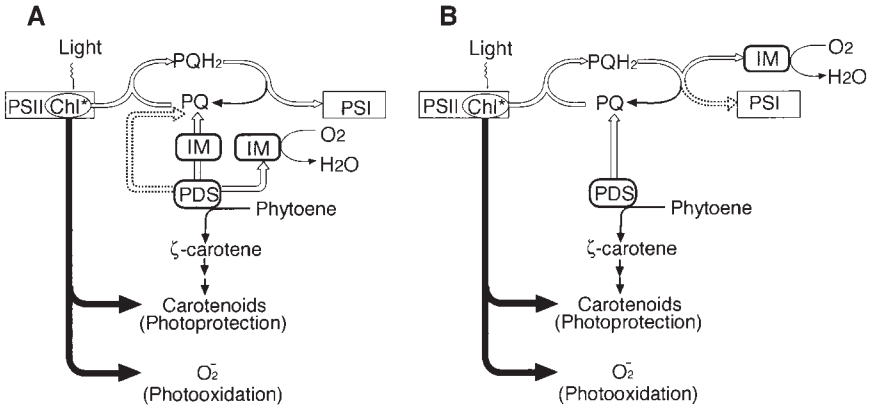


**Figure 6.** Two Working Models of *im* Variegation.

Light is absorbed by the light-harvesting complex of photosystem II (PSII), and energy from excited state chlorophyll (Chl*) can either be transferred to the reaction center or used to form triplet chlorophyll. Unless quenched by colored carotenoids, energy from triplet chlorophyll generates oxygen radicals ($O_2^-$), which can lead to the photooxidation of the contents of the plastid if not detoxified by free radical scavengers (such as superoxide dismutase). The pathway of energy flow from triplet chlorophyll is indicated by shaded arrows, and the pathway of electron transport from PSII via the plastoquinone pool (PQ) to photosystem I (PSI) is shown as an open arrow. Electrons also can enter the PQ pool by the PDS-mediated desaturation of phytoene. In **(A)**, IM acts as a cofactor of PDS and mediates an efficient transfer of electrons to the PQ pool or to molecular oxygen. However, electrons also may be transferred directly from PDS to the PQ pool (broken arrow) in an inefficient "redundant" process that is responsible for the generation of green plastids in null *im* plants. In **(B)**, PDS transfers electrons from phytoene to the PQ pool, and IM acts after this step to reduce molecular oxygen. In the absence of IM, electron flow from the PQ pool to PSI serves as the redundant function to generate green plastids.

### The Revised Threshold Model of Variegation: Electron Transport Capacity for Phytoene Desaturation

In an earlier model of *im* variegation (Wetzel et al., 1994), we hypothesized that the mutation rendered the IM gene product light-labile (but still partially functional) and that a threshold of IM activity was required for normal chloroplast development. In the mutant, we assumed that the higher the light intensity, the fewer the plastids with the requisite threshold and hence the greater the extent of white sector formation. We have amended our hypothesis in light of our finding that the three *im* alleles we have sequenced (*spotty*, *CS3157*, and *im-1*) are most likely null, and therefore, no *IM* gene product is present for light-induced destruction. Taken together with the fact that *im* plants are heteroplastidic and variegated, not albino, the finding of null *im* alleles suggests that there is a redundant function that is able to compensate for the absence of IM activity in the green plastids. Low-stringency hybridizations have failed to detect *IM*-related sequences in the Arabidopsis genome (data not shown), and hence the redundant or parallel redox component is unlikely to be another IM-like AOX protein. As illustrated in Figure 6A, one possibility is that the redundant function is inefficient transfer of electrons from PDS to the plastoquinone pool. In Figure 6B, the redundant function is illustrated as electron flow to photosystem I.

Carotenoids act as nonphotochemical quenchers of excess light energy absorbed by light-harvesting complexes (e.g., reviewed in Demmig-Adams et al., 1996). In the absence of a sufficient level of free-radical scavenging mechanisms (such as may occur during the early stages of chloroplast biogenesis), unquenched excess light energy leads to the formation of harmful active oxygen species and to photooxidation of the contents of the plastid. Photooxidative damage appears to be localized to the plastid compartment (Oelmüller, 1989). As revised, our model invokes a threshold of electron transport capacity for phytoene desaturation that is required for carotenoid synthesis and the development of green chloroplasts. Below this threshold, carotenoids cannot be made in sufficient quantity to prevent light-induced photodestruction.

According to our model, different pathways of electron transport function in phytoene desaturation at different stages of development and with different efficiencies, depending on which electron transport components are available. A fundamental assumption is that IM is one of these components and is required for carotenoid synthesis during early chloroplast biogenesis, that is, when thylakoid membranes are being elaborated in growing chloroplasts, after division of either progenitor proplastids in the meristem or mature chloroplasts in the expanding leaf (reviewed in Mullet, 1988). Although we have not yet examined IM ex-

pression during leaf development, this assumption would be consistent with our observation that IM is expressed early in cotyledon development (Wetzel et al., 1994).

We hypothesize that PDS would be unable or only minimally able to perform phytoene desaturation during the early stages of thylakoid development when IM is absent and the alternative pathway is either inefficient (Figure 6A) or not yet fully functional (Figure 6B). Phytoene would accumulate either because electrons could not be transferred quickly enough to the plastoquinone pool by the inefficient path (Figure 6A) or because the plastoquinone pool was overreduced (Figure 6B). In either of these cases, carotenoid synthesis would be blocked, and the plastids would be in a state vulnerable to high light–induced photooxidation by newly accumulating chlorophylls. In essence, a developmental race would occur between, on the one hand, photooxidation due to a lack of carotenoid photoprotection, and on the other hand, the development of an efficient mechanism of electron transport away from phytoene to accommodate PDS activity and the synthesis of enough carotenoids to afford photoprotection. Low light and thus lower photooxidative pressure would allow more plastids to survive the race through the vulnerable stage, accumulate chlorophylls, and turn green. In the presence of functional IM, electron transport would not be inhibited during early development, and carotenoid synthesis would proceed unhindered, thus avoiding photooxidative vulnerability.

In sum, the outcome of development in IM-deficient plastids is either a white, photooxidized state or a fully functional green state. If the inner membrane structure has been destroyed along with the resident pigments, then there will be no electron transport from phytoene and consequently no carotenoid synthesis (white plastids). If, on the other hand, enough electron transfer from phytoene can occur to support colored carotenoid accumulation, then wild-type levels of pigments can accumulate, as observed in green *im* plastids and cells (Wetzel et al., 1994; Meehan et al., 1996). White plastids appear to be capable of division because the requisite components are imported from the nucleus–cytoplasm (Tilney-Bassett, 1975). Therefore, the *im* mutation is effectively plastid autonomous, and each round of plastid division and differentiation carries the same risks of photooxidation.

### Tissue-Level Patterns of Variegation

The model we have described explains the development of white plastids at the organelle level, but the phenotype of *im* manifests itself as tissue-level sectoring. Several factors may be important in determining this patterning. One factor is the light environment. In developing leaves, cells and young plastids do not receive uniform levels of illumination, and the light environment can be affected by the angle of incident light, the presence of shading structures, and the amount of light that penetrates through the tissue layers (reviewed in Smith et al., 1997). One may expect, however, that neighboring cells in areas of leaf development would be subject to relatively similar levels of illumination due to their physical proximity. Thus, even though there would be a range of light levels at the organelle level, the overall difference between a level of light sufficient for the photooxidation of carotenoid-deficient plastids and that permissive for normal chloroplast development may be realized only on sections, or sectors, of cells. In this case, the pattern of variegation would be determined by the light environment. Clearly, higher overall incident light intensities would shift more mutant cells into the photooxidation range.

A second factor that may be important in determining tissue-wide patterns of variegation is related to the amount of existing thylakoid material that is passed into nascent plastids from their progenitors. When white plastids divide, the daughters are especially vulnerable to photooxidation because they have no electron transport capacity to start with for even minimal PDS function. White plastids are propagated forming a clone of cells (a white sector) until, for example, light intensities are lowered. Lower light would decrease the threshold of carotenoid synthesis required for photoprotection, allowing electron transport capacity to develop, phytoene to be desaturated, and carotenoid synthesis to occur. A green plastid (or cell) could then be formed. In like manner, green chloroplasts in mutant tissue do not have wild-type capacity for electron transport and PDS activity; thus, if put under high enough light, they are still susceptible to photooxidation during their vulnerable stage, leading to white sectors arising from green.

A third factor that may affect sectoring is related to the abundance and activities of components of carotenoid biosynthesis—electron transport and radical scavenging. These may be expressed in a cell-specific manner, resulting in a pattern of variegation that is usually obscured. Considered together, our data point toward the notion that tissue-wide patterns of variegation in *im* are probably due to a complex interplay of factors. Future studies of *im* should provide much information concerning these mechanisms.

## METHODS

### Plant Material

The *spotty* allele of *immutans* (*im*) has been described previously (Wetzel et al., 1994). We found that plants carrying this allele, in contrast to other *im* mutants, are fast growing and easy to cross (S. Rodermel and C. Wetzel, unpublished data); this allele was provided to the Carol group for timely crosses to verify that their *Activator*-tagged mutation was, indeed, in the *IM* gene (Carol et al., 1999). For our positional cloning experiments, an $F_2$ mapping population was generated by crossing the *spotty* allele (in an *Arabidopsis thaliana* ecotype Columbia background) with a Landsberg *erecta* chromosome 4 marker strain (*cer2*/*ap2*/*bp2*) (Koornneef et al., 1983). A total of 2495 $F_2$ plants (4990 chromosomes) were analyzed to generate the recombinant pool. The *im-1* allele (Rédei, 1967) was obtained

from G.P. Rédei (University of Missouri, Columbia). The *CS3157* allele was obtained from the Arabidopsis Biological Resource Center (Ohio State University, Columbus) and was originally in the mutant collection of G.P. Rédei. *im-1* and *CS315*7 are both in the Columbia background.

### DNA Manipulations

Several types of libraries were used in the positional cloning of *im.* These included four yeast artificial chromosome (YAC) libraries (Ecker, 1990; Ward and Jen, 1990; Grill and Somerville, 1991; Creusot et al., 1995), the TAMU bacterial artificial chromosome (BAC) library (Choi et al., 1995), the pOCA18 cosmid library (Olszewski et al., 1988), and λPRL2, a cDNA library made with mRNA from various Arabidopsis tissues and at different stages of development (Newman et al., 1994). All of these resources came from the Arabidopsis Biological Resource Center. Protocols for the manipulation of these libraries are described in the references cited above as well as by Schmidt et al. (1996) and Ausubel et al. (1998). These include procedures for library and clone maintenance, the isolation of DNAs, and library screening. Sizes of YAC and BAC clones were determined by pulsed-field gel electrophoresis (Schmidt et al., 1996).

The ends of YAC, BAC, and cosmid inserts were isolated for use both as probes and as markers in the chromosome walk. YAC left ends were isolated by plasmid rescue (Schmidt et al., 1996), and YAC right ends were isolated by *pyrF* complementation (Wright et al., 1997). BAC and cosmid end clones were isolated by inverse polymerase chain reaction (PCR) or by direct subcloning. Established methods were used for PCR, inverse PCR, and long PCR (Ausubel et al., 1998). For DNA gel blot and colony hybridizations, the cloned DNAs were labeled by random priming (Ausubel et al., 1998) and hybridized with filters containing YACs, BACs, or cosmids or with filters containing Arabidopsis genomic DNA. Hybridization and Arabidopsis DNA isolation procedures were as described by Wetzel et al. (1994).

The cloned YAC, BAC, and cosmid ends were used to generate cleaved amplified polymorphic sequence (CAPS) markers (Konieczny and Ausubel, 1993) for use in mapping the end clones with respect to *im.* CAPS markers also were generated from random EcoRI subfragments of YAC CIC7H1 cloned into pBluescript SK− (Stratagene, La Jolla, CA). Other polymorphic sequences that were used in the chromosome walk included LM117, a restriction fragment length polymorphism marker (Mindrinos et al., 1994), and two simple sequence length polymorphism markers, *nga1111* and *nga1139* (Bell and Ecker, 1994).

DNA sequencing was performed by the Iowa State University Nucleic Acids Facility. DNA sequences were analyzed using the Genetics Computer Group (Madison, WI) software package (Devereux et al., 1984). Phylogenetic analyses were conducted by the neighbor-joining algorithm using Phylip (Saitou and Nei, 1987; Felsenstein, 1993). The *IM* wild-type cDNA sequence has been submitted to the DDBJ, EMBL, and GenBank databases as accession number AF098072.

### RNA Manipulations

Procedures for the isolation of *im* and wild-type RNA and for reverse transcriptase–PCR (RT-PCR) are described by Wetzel and Rodermel (1998). 5′ rapid amplification of cDNA ends (5′ RACE) was performed using the 5′ RACE system, version 2.0 (Gibco BRL).

### ACKNOWLEDGMENTS

We thank the Arabidopsis Biological Resource Center for providing many of the reagents for the chromosome walk and G.P. Rédei for providing several *im* alleles. We also thank Renate Schmidt and Caroline Dean (John Innes Centre, Norwich, UK) for providing, before publication, YAC clones that reside in the vicinity of *im* (Schmidt et al., 1996) and LeAnn Meehan for assistance in the chromosome walk. We very much appreciate the helpful comments made on our manuscript by three anonymous reviewers and by Dr. David Oliver and Dr. Marc Anderson (Iowa State University). This is journal paper No. J-18142 of the Iowa Agricultural Experiment Station, project 2987. This work was supported by funding from the U.S. Department of Energy (Grant No. DE-FG02-94ER20147) to S.R. and D.F.V.

Received July 22, 1998; accepted November 3, 1998.

### REFERENCES

**Al-Babili, S., Lintig, J.V., Haubruck, H., and Beyer, P.** (1996). A novel, soluble form of phytoene desaturase from *Narcissus pseudonarcissus* chromoplasts is Hsp70-complexed and competent for flavination, membrane association and enzymatic activation. Plant J. **9,** 601–612.

**Ausubel, F.M., Brent, R., Kingston, R.E., Moore, D.D., Seidman, J.G., Smith, J.A., and Struhl, K.,** eds (1998). Current Protocols in Molecular Biology. (New York: Greene Publishing Associates/ Wiley Interscience).

**Bartley, G.E., Viitanen, P.V., Pecker, I., Chamovitz, D., Hirschberg, J., and Scolnik, P.A.** (1991). Molecular cloning and expression in photosynthetic bacteria of a soybean cDNA coding for phytoene desaturase, an enzyme of the carotenoid biosynthetic pathway. Proc. Natl. Acad. Sci. USA **88,** 6532–6536.

**Bell, C.J., and Ecker, J.R.** (1994). Assignment of 30 microsatellite loci to the linkage map of *Arabidopsis.* Genomics **19,** 137–144.

**Beyer, P., Mayer, M., and Kleinig, H.** (1989). Molecular oxygen and the state of geometric isomerism of intermediates are essential in the carotene desaturation and cyclization reactions in daffodil chromoplasts. Eur. J. Biochem. **184,** 141–150.

**Bonk, M., Tadros, M., Vandekerckhove, J., Al-Babili, S., and Beyer, P.** (1996). Purification and characterization of chaperonin 60 and heat-shock protein 70 from chromoplasts of *Narcissus pseudonarcissus.* Plant Physiol. **111,** 931–939.

**Brendel, V., Kleffe, J., Carle-Urioste, J.C., and Walbot, V.** (1998). Prediction of splice sites in plant pre-mRNA from sequence properties. J. Mol. Biol. **276,** 85–104.

**Büchel, C., and Garab, G.** (1997). Respiratory regulation of electron transport in chloroplasts: Chlororespiration. In Handbook of Photosynthesis, M. Pessarakli, ed (New York: Marcel Dekker, Inc.), pp. 83–93.

**Burrows, P.A., Sazanov, L.A., Svab, Z., Maliga, P., and Nixon, P.J.** (1998). Identification of a functional respiratory complex in chloroplasts through analysis of tobacco mutants containing disrupted plastid *ndh* genes. EMBO J. **17,** 868–876.

**Carol, P., Stevenson, D., Bisanz, C., Breitenbach, J., Sandmann, G., Mache, R., Coupland, G., and Kuntz, M.** (1999). Mutations in the Arabidopsis gene *IMMUTANS* cause a variegated phenotype by inactivating a chloroplast terminal oxidase associated with phytoene desaturation. Plant Cell **11,** 57–68.

**Choi, S., Creelman, R.A., Mullet, J.E., and Wing, R.A.** (1995). Construction and characterization of a bacterial artificial chromosome library of *Arabidopsis thaliana.* Weeds World **2,** 17–20.

**Cline, K., and Henry, R.** (1996). Import and routing of nucleus-encoded chloroplast proteins. Annu. Rev. Cell Dev. Biol. **12,** 1–26.

**Creusot, F., Fouilloux, E., Dron, M., Lafleuriel, J., Picard, G., Billault, A., LePaslier, D., Cohen, D., Chaboute, M., Durr, A., Fleck, J., Gigot, C., Camilleri, C., Bellini, C., Caboche, M., and Bouchez, D.** (1995). The CIC library: A large insert YAC library for genome mapping in *Arabidopsis thaliana.* Plant J. **8,** 763–770.

**Cunningham, F.X., and Gantt, E.** (1998). Genes and enzymes of carotenoid biosynthesis in plants. Annu. Rev. Plant Physiol. Plant Mol. Biol. **49,** 557–583.

**Demmig-Adams, B., Gilmore, A.M., and Adams III, W.W.** (1996). In vivo functions of carotenoids in higher plants. FASEB J. **10,** 403–412.

**Devereux, J., Haeberli, P., and Smithies, O.** (1984). A comprehensive set of sequence analysis programs for the VAX. Nucleic Acids Res. **12,** 387–395.

**Ecker, J.R.** (1990). PFGE and YAC analysis of the *Arabidopsis* genome. Methods Companion Methods Enzymol. **1,** 186–194.

**Feild, T.S., Nedbal, L., and Ort, D.R.** (1998). Nonphotochemical reduction of the plastoquinone pool in sunflower originates from chlororespiration. Plant Physiol. **116,** 1209–1218.

**Felsenstein, J.** (1993). PHYLIP (Phylogeny Inference Package). (Seattle, WA: University of Washington).

**Giuliano, G., Bartley, G.E., and Scolnik, P.A.** (1993). Regulation of carotenoid biosynthesis during tomato development. Plant Cell **5,** 379–387.

**Granick, S.** (1955). Die plastiden und chondriosomen. In Encyclopedia of Plant Physiology, Vol. 1, W. Ruhland, ed (Berlin: Springer-Verlag), pp. 507–564.

**Grill, E., and Somerville, C.** (1991). Construction and characterization of a yeast artificial chromosome library of *Arabidopsis* which is suitable for chromosome walking. Mol. Gen. Genet. **226,** 484–490.

**Gu, J., Miles, D., and Newton, K.J.** (1993). Analysis of leaf sectors in the NCS6 mitochondrial mutant of maize. Plant Cell **5,** 963–971.

**Han, C.-D., and Martienssen, R.A.** (1995). The *iojap* protein (IJ) is associated with 50S chloroplast ribosomal subunits. Maize Coop. Newsl. **69,** 32.

**Han, C.-D., Coe, E.H., Jr., and Martienssen, R.A.** (1992). Molecular cloning and characterization of *iojap* (*ij*), a pattern striping gene of maize. EMBO J. **11,** 4037–4046.

**Hess, W.R., Müller, A., and Börner, T.** (1994). Ribosome-deficient plastids affect transcription of light-induced nuclear genes: Genetic evidence for a plastid-derived signal. Mol. Gen. Genet. **242,** 305–312.

**Hoefnagel, M.H.N., Millar, A.H., Wiskich, J.T., and Day, D.A.** (1995). Cytochrome and alternative respiratory pathways compete for electrons in the presence of pyruvate in soybean mitochondria. Arch. Biochem. Biophys. **318,** 394–400.

**Hugueney, P., Römer, S., Kuntz, M., and Camara, B.** (1992). Characterization and molecular cloning of a flavoprotein catalyzing the synthesis of phytofluene and zeta-carotene in *Capsicum* chromoplasts. Eur. J. Biochem. **209,** 399–407.

**Jäger-Vottero, P., Dorne, A.-J., Jordanov, J., Douce, R., and Joyard, J.** (1997). Redox chains in chloroplast envelope membranes: Spectroscopic evidence for the presence of electron carriers, including iron-sulfur centers. Proc. Natl. Acad. Sci. USA **94,** 1597–1602.

**Kofer, W., Koop, H.-U., Wanner, G., and Steinmüller, K.** (1998). Mutagenesis of the genes encoding subunits A, C, H, I, J and K of the plastid NAD(P)H-plastoquinone-oxidoreductase in tobacco by polyethylene glycol–mediated plastome transformation. Mol. Gen. Genet. **258,** 166–173.

**Konieczny, A., and Ausubel, F.** (1993). A procedure for quick mapping of *Arabidopsis* mutants using ecotype specific markers. Plant J. **4,** 403–410.

**Koornneef, M., van Eden, J., Hanhart, C.J., Stam, P., Braaksma, F.J., and Feenstra, W.J.** (1983). Linkage map of *Arabidopsis thaliana.* J. Hered. **74,** 265–272.

**Kreuz, K., Beyer, P., and Kleinig, H.** (1982). The site of carotenogenic enzymes in chromoplasts from *Narcissus pseudonarcissus* L. Planta **154,** 66–69.

**Kumar, A.M., and Söll, D.** (1992). *Arabidopsis* alternative oxidase sustains *Escherichia coli* respiration. Proc. Natl. Acad. Sci. USA **89,** 10842–10846.

**Lauer, M., Knudsen, C., Newton, K.J., Gabay-Laughnan, S., and Laughnan, J.R.** (1990). A partially deleted mitochondrial cytochrome oxidase gene in the NCS6 abnormal growth mutant of maize. New Biol. **2,** 179–186.

**Martínez-Zapater, J.M.** (1992). Genetic analysis of variegated mutants in *Arabidopsis.* J. Hered. **84,** 138–140.

**Martínez-Zapater, J.M., Gil, P., Capel, J., and Somerville, C.R.** (1992). Mutations at the Arabidopsis *CHM* locus promote rearrangements of the mitochondrial genome. Plant Cell **4,** 889–899.

**Mayer, M.P., Beyer, P., and Kleinig, H.** (1990). Quinone compounds are able to replace molecular oxygen as terminal electron acceptor in phytoene desaturation in chromoplasts of *Narcissus pseudonarcissus* L. Eur. J. Biochem. **191,** 359–363.

**Mayer, M.P., Nievelstein, V., and Beyer, P.** (1992). Purification and characterization of a NADPH dependent oxidoreductase from chromoplasts of *Narcissus pseudonarcissus*: A redox-mediator possibly involved in carotene desaturation. Plant Physiol. Biochem. **30,** 389–398.

**Meehan, L., Harkins, K., Chory, J., and Rodermel, S.** (1996). *Lhcb* transcription is coordinated with cell size and chlorophyll accumulation. Plant Physiol. **112,** 953–963.

**Mindrinos, M., Katagiri, F., Yu, G.L., and Ausubel, F.M.** (1994). The A. thaliana disease resistance gene *RPS2* encodes a protein containing a nucleotide-binding site and leucine-rich repeats. Cell **78,** 1089–1099.

**Moore, A.L., Umbach, A.L., and Siedow, J.N.** (1995). Structure–function relationships of the alternative oxidase of plant mitochondria: A model of the active site. J. Bioenerg. Biomembr. **27,** 367–377.

**Mullet, J.E.** (1988). Chloroplast development and gene expression. Annu. Rev. Plant Physiol. Plant Mol. Biol. **39,** 475–502.

**Nakai, K., and Kanehisa, M.** (1992). A knowledge base for predicting protein localization sites in eukaryotic cells. Genomics **14,** 897–911.

**Newman, T., de Bruijn, F.J., Green, P., Keegstra, K., Kende, H., McIntosh, L., Ohlrogge, J., Raikhel, N., Somerville, S., Thomashow, M., Retzel, E., and Somerville, C.** (1994). Genes galore: A summary of methods for accessing results from large-scale partial sequencing of anonymous *Arabidopsis* cDNA clones. Plant Physiol. **106,** 1241–1255.

**Nievelstein, V., Vandekerckhove, J., Tadros, M.H., von Lintig, J., Nitschke, W., and Beyer, P.** (1995). Carotene desaturation is linked to a respiratory redox pathway in *Narcissus pseudonarcissus* chromoplast membranes: Involvement of a 23-kDa oxygen-evolving-complex-like protein. Eur. J. Biochem. **233,** 864–872.

**Norris, S.R., Barrette, T.R., and DellaPenna, D.** (1995). Genetic dissection of carotenoid synthesis in Arabidopsis defines plastoquinone as an essential component of phytoene desaturation. Plant Cell **7,** 2139–2149.

**Oelmüller, R.** (1989). Photooxidative destruction of chloroplasts and its effect on nuclear gene expression and extraplastidic enzyme levels. Photochem. Photobiol. **49,** 229–239.

**Olszewski, N.E., Martin, F.B., and Ausubel, F.M.** (1988). Specialized binary vector for plant transformation: Expression of the *Arabidopsis thaliana* AHAS gene in *Nicotiana tabacum*. Nucleic Acids Res. **16,** 10765–10782.

**Purvis, A.C., and Shewfelt, R.L.** (1993). Does the alternative pathway ameliorate chilling injury in sensitive plant tissues? Physiol. Plant. **88,** 712–718.

**Rédei, G.P.** (1963). Somatic instability caused by a cysteine-sensitive gene in *Arabidopsis.* Science **139,** 767–769.

**Rédei, G.P.** (1967). Biochemical aspects of a genetically determined variegation in *Arabidopsis.* Genetics **56,** 431–443.

**Rédei, G.P.** (1973). Extra-chromosomal mutability determined by a nuclear gene locus in *Arabidopsis.* Mutat. Res. **18,** 149–162.

**Rédei, G.P.** (1975). *Arabidopsis* as a genetic tool. Annu. Rev. Genet. **9,** 111–127.

**Ribas-Carbo, M., Berry, J.A., Yakir, D., Giles, L., Robinson, S.A., Lennon, A.M., and Siedow, J.N.** (1995). Electron partitioning between the cytochrome and alternative pathways in plant mitochondria. Plant Physiol. **109,** 829–837.

**Röbbelen, G.** (1968). Genbedingte Rotlicht-Empfindlichkeit der Chloroplastendifferenzierung bei *Arabidopsis.* Planta **80,** 237–254.

**Rost, B., Casadio, R., Fariselli, P., and Sander, C.** (1995). Prediction of helical transmembrane segments at 95% accuracy. Prot. Sci. **4,** 521–533.

**Rousell, D.L., Thompson, D.L., Pallardy, S.G., Miles, D., and Newton, K.J.** (1991). Chloroplast structure and function is altered in the NCS2 maize mitochondrial mutant. Plant Physiol. **96,** 232–238.

**Saisho, D., Nambara, E., Naito, S., Tsutsumi, N., Hirai, A., and Nakazono, M.** (1997). Characterization of the gene family for alternative oxidase from *Arabidopsis thaliana.* Plant Mol. Biol. **35,** 585–596.

**Saitou, N., and Nei, M.** (1987). The neighbor-joining method: A new method for reconstructing phylogenetic trees. Mol. Biol. Evol. **4,** 406–425.

**Sakamoto, W., Kondo, H., Murata, M., and Motoyoshi, F.** (1996). Altered mitochondrial gene expression in a maternal distorted leaf mutant of Arabidopsis induced by *chloroplast mutator.* Plant Cell **8,** 1377–1390.

**Sandmann, G., and Böger, P.** (1989). Inhibition of carotenoid biosynthesis by herbicides. In Target Sites of Herbicide Action, P. Böger and G. Sandmann, eds (Boca Raton, FL: CRC Press), pp. 25–44.

**Schmidt, R., West, J., Cnops, G., Love, K., Balestrazzi, A., and Dean, C.** (1996). Detailed description of four YAC contigs representing 17 Mb of chromosome 4 of *Arabidopsis thaliana* ecotype Columbia. Plant J. **9,** 755–765.

**Schulz, A., Ort, O., Beyer, P., and Kleinig, H.** (1993). SC-0051, a 2-benzoyl-cyclohexane-1,3-dione bleaching herbicide, is a potent inhibitor of the enzyme *p*-hydroxyphenylpyruvate dioxygenase. FEBS Lett. **318,** 162–166.

**Scolnik, P.A., Hinton, P., Greenblatt, I.M., Giuliano, G., Delanoy, M.R., Spector, D.L., and Pollock, D.** (1987). Somatic instability of carotenoid biosynthesis in the tomato *ghost* mutant and its effect on plastid development. Planta **171,** 11–18.

**Shikanai, T., Endo, T., Hasimoto, T., Yamada, Y., Asada, K., and Yokota, A.** (1998). Directed disruption of the tobacco *ndhB* gene impairs cyclic electron flow around photosystem I. Proc. Natl. Acad. Sci. USA **95,** 9705–9709.

**Siedow, J.N., and Umbach, A.L.** (1995). Plant mitochondrial electron transfer and molecular biology. Plant Cell **7,** 821–831.

**Siedow, J.N., Umbach, A.L., and Moore, A.L.** (1995). The active site of the cyanide-resistant oxidase from plant mitochondria contains a binuclear iron center. FEBS Lett. **362,** 10–14.

**Smith, W.K., Vogelmann, T.C., DeLucia, E.H., Bell, D.T., and Shepherd, K.A.** (1997). Leaf form and photosynthesis. BioScience **47,** 785–793.

**Taylor, W.C.** (1989). Regulatory interactions between nuclear and plastid genomes. Annu. Rev. Plant Physiol. Plant Mol. Biol. **40,** 211–233.

**Tilney-Bassett, R.A.E.** (1975). Genetics of variegated plants. In Genetics and Biogenesis of Mitochondria and Chloroplasts, C.W. Birky, P.S. Perlman, and T.J. Byers, eds (Columbus, OH: Ohio State University Press), pp. 268–308.

**Umbach, A.L., and Siedow, J.N.** (1993). Covalent and noncovalent dimers of the cyanide-resistant alternative oxidase protein in higher plant mitochondria and their relationship to enzyme activity. Plant Physiol. **103,** 845–854.

**Umbach, A.L., and Siedow, J.N.** (1996). The reaction of the soybean cotyledon mitochondrial cyanide-resistant oxidase with sulf-

hydryl reagents suggests that α-keto acid activation involves the formation of a thiohemiacetal. J. Biol. Chem. **271,** 25019–25026.

**Vanlerberghe, G.C., and McIntosh, L.** (1997). Alternative oxidase: From gene to function. Annu. Rev. Plant Physiol. Plant Mol. Biol. **48,** 703–734.

**Vanlerberghe, G.C., Vanlerberghe, A.E., and McIntosh, L.** (1997). Molecular genetic evidence of the ability of alternative oxidase to support respiratory carbon metabolism. Plant Physiol. **113,** 657–661.

**Walbot, V., and Coe, E.H.** (1979). Nuclear gene *iojap* conditions a programmed change to ribosome-less plastids in *Zea mays.* Proc. Natl. Acad. Sci. USA **76,** 2760–2764.

**Ward, E.R., and Jen, G.C.** (1990). Isolation of single-copy-sequence clones from a yeast artificial chromosome library of randomly-sheared *Arabidopsis thaliana* DNA. Plant Mol. Biol. **14,** 561–568.

**Wetzel, C.M., and Rodermel, S.** (1998). Regulation of phytoene desaturase expression is independent of leaf pigment content in *Arabidopsis thaliana.* Plant Mol. Biol. **37,** 1045–1053.

**Wetzel, C.M., Jiang, C.-Z., Meehan, L.J., Voytas, D.F., and Rodermel, S.R.** (1994). Nuclear–organelle interactions: The *immutans* variegation mutant of *Arabidopsis* is plastid autonomous and impaired in carotenoid biosynthesis. Plant J. **6,** 161–175.

**Wright, D.A., Park, S.-K., Wu, D., Phillips, G.J., Rodermel, S.R., and Voytas, D.F.** (1997). Recovery of YAC-end sequences through complementation of an *Escherichia coli pyrF* mutation. Nucleic Acids Res. **25,** 2679–2680.